Available online at www.sciencedirect.com
ScienceDirect
Trans. Nonferrous Met. Soc. China 25(2015) 1080−1090
Transactions of Nonferrous Metals Society of China
www.tnmsc.cn

Microstructure and tensile properties of friction stir welded dissimilar AA6061−AA5086 aluminium alloy joints

M. ILANGOVAN[1], S. RAJENDRA BOOPATHY[1], V. BALASUBRAMANIAN[2]

1. Department of Mechanical Engineering, College of Engineering Guindy, Anna University, Chennai. India;
2. Center for Materials Joining & Research, Department of Manufacturing Engineering, Annamalai University, Annamalai Nagar Chidambaram 608002, Tamilnadu, India

Received 30 April 2014; accepted 3 November 2014

Abstract: The fusion welding of dissimilar heat treatable and non-heat treatable aluminium alloy faced many problems related to solidification. The difficulties can be overcome to achieve the combined beneficial properties of both aluminium alloys using friction stir welding (FSW). The microstructural features and tensile properties of friction stir welded (FSW) similar and dissimilar joints made of AA6061 and AA5086 aluminium alloys were investigated. The microstructures of various regions were observed and analyzed by means of optical and scanning electron microscopy. Microhardness was measured at various zones of the welded joints. The tensile properties of the joints were evaluated and correlated with the microstructural features and microhardness values. The dissimilar joint exhibits a maximum hardness of HV 115 and a joint efficiency of 56%. This was attributed to the defect free stir zone formation and grain size strengthening.

Key words: friction stir welding; dissimilar joint; aluminium alloy; microstructure; tensile strength

1 Introduction

Many specific properties of aluminum alloys including light weight, good structural strength, superior corrosion resistance enable them to be applied for structural parts. The demand of aircraft and automotive industries for lightweight materials is met by aluminum alloys [1]. The aluminum alloys AA6xxx (heat treatable) and AA5xxx (non-heat treatable) are extensively used in the fabrication of aircraft structures, ship structures, transport vehicles and other structural members [2,3]. Welding of these two different grades of aluminium alloys arise in a few situations where high strength and high corrosion resistance are required such as marine structures. AA6061 alloy is better known for its strength but AA5086 alloy is known for its corrosion resistance. In ship hull structures, the structures/frames exposed to the sea water are made by AA5086 alloy to give better corrosion resistance but the inner structures/frames not exposed to sea water are made by AA6061 alloy to give improved strength.

Under these situations, joining of these two grades of alloys in a structural member is inevitable. However, joining of these two grades of aluminium alloys by conventional fusion welding techniques such as gas tungsten arc welding (GTAW) and gas metal arc welding (GMAW) processes are cumbersome due to non-availability of matching filler metals and the difference in solidification mode due to the variation in chemical compositions. Therefore, solid state joining technique is highly recommended to overcome these problems [4−6]. Friction stir welding (FSW) is an appropriate solid state welding technique to join any combination of dissimilar aluminum alloys effectively [7−10]. FSW process does not require any filler metal additions since it is an autogenous, hot shear process in principle, uses a non-consumable tool (harder than aluminium alloys) to plasticize and stir the materials to transport from one end to other end thus making a sound joint possible. Moreover, the frictional heat generated by the rotating tool during welding process raises the temperature of the materials to be joined to the level well below its melting point (100 °C less) and hence no melting takes place. This eliminates solidification related problems such as porosity, hot cracking, alloy segregation and partially melting zone.

FSW was used to join various dissimilar combination

Corresponding author: M. ILANGOVAN; E-mail: ilaango@gmail.com
DOI: 10.1016/S1003-6326(15)63701-3

like join Al to Mg [11], Al to Cu [12], Al to steel [13]. All these investigations concluded that the formation of the brittle intermetallic compounds in the stir zone is unavoidable while joining dissimilar materials and results in inferior mechanical properties. Recently, several attempts have been made to tailor the interfaces of dissimilar materials to optimize the strength [14,15]. FSW of dissimilar AA5xxx and AA6xxx joints was investigated by HECTOR et al [16] and reported that FSW process can join dissimilar aluminium material of higher tensile strength. KHODIR and SHIBAYANAGI [17] investigated the friction stir welded dissimilar aluminum joints of 2024−T351 alloy and 6056−T4 and found that the tensile fracture occurred in the stir zone due to the annealing effect which made the region weaker. CAM et al [18] investigated the FSW of the non heat-treatable Al−5086 H32 Al alloys. Defect free joint was achieved at tool rotational speed of 1600 r/min and tool-traversing speeds of 175, 200, and 225 mm/min. They observed that the loss of cold-work hardening occurred in the stir zone and the tensile fracture occurred at the stir zone. This failure was mainly attributed to heat generation during FSW. Hence, the optimum heat generation is mandatory in FSW to attain defect free stir zone, higher strength and hardness.

Lot of investigations have been carried out to understand the evolution of microstructural features and the tensile properties of friction stir welded similar joints of AA6061 and AA5086 aluminium alloys [19−21]. But the published information on FSW of dissimilar grades of aluminum alloys is very scant and hence the understanding on the microstructural evolution of dissimilar grades of aluminium alloys in the stir zone is very limited. Hence, in this investigation, an attempt is made to join 6 mm thick aluminum alloys of AA6061 and AA5086 grades using FSW process to understand the evolution of microstructure in the stir zone and its influence on tensile properties of the joints.

2 Experimental

A joint configuration of 150 mm × 100 mm ×6 mm plate was used for friction stir welding. The parent metal AA6061 is solution treated and artificially aged and the parent metal AA5086 is annealed. The chemical composition and mechanical properties of the parent materials are listed in Tables 1 and 2, respectively. In this work, three different joints are made by computer numerically controlled friction stir welding machine and these joints are referred by following notification throughout the manuscript: 1) SS66 (AA6061 and AA5086), 2) SS5 (AA5086 with AA5086), 3) D65 (AA6061 with AA5086). The welding parameters used to fabricate the joints are presented in Table 3. The specimens were extracted using a power hacksaw and then machined to the required dimensions along the transverse direction from the FSWed plate to carry out microstructural characterization. The specimens were prepared as per ASTM standard E407 metallographic procedure. Modified Keller reagent and Wecks reagent were used to reveal the microstructure. The material flow, grain size and grain orientations were carried out using an optical microscope. ASTM E8M-04 guidelines were followed in preparing the tensile specimens. Tensile test was carried out in 100 kN electro-mechanical controlled universal testing machine (Maker: FIE, India; Model: UNITECH 94001). The tensile specimen was loaded at the constant strain rate of 1.5 kN/min as per ASTM specifications. Three tensile specimens from each joint were prepared and tested, and the average value was taken for analysis. The 0.2% offset yield strength, ultimate tensile strength, percentage of elongation and joint efficiency were evaluated from unnotched (smooth) tensile specimen (Fig. 1(a)). Notch tensile strength and notch strength ratio were evaluated by introducing notch in the standard smooth tensile specimen (Fig. 1(b)). The fractured surfaces of tensile test specimens were analysed using scanning electron microscope (SEM). A Vickers microhardness tester (SHIMADZU, Japan; model HMV−2T) was employed for measuring the hardness across the transverse cross section of the various zones of FSW joint using a load of 50 g and dwell time of 15 s.

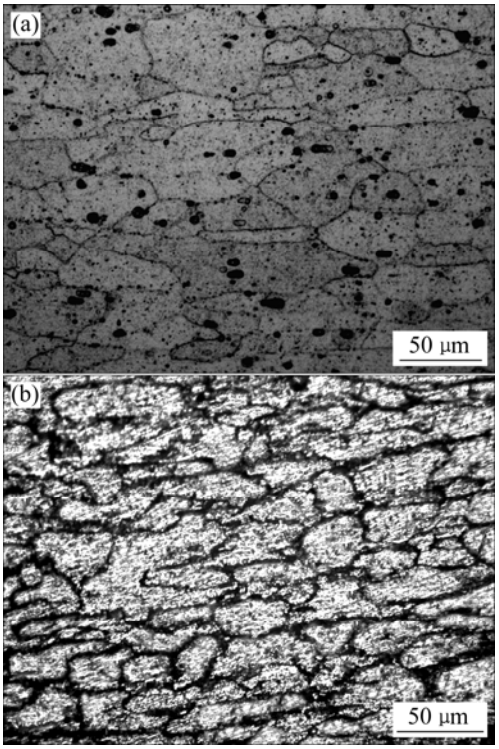

Fig. 1 Optical micrographs of parent materials: (a) AA6061 Al alloy; (b) AA5086 Al alloy

Table 1 Chemical composition of parent materials (mass fraction, %)

Alloy	Mg	Mn	Cu	Cr	Si	Fe	Al
AA6061−T6	1.20	0.15	0.20	0.04	0.60	0.75	Bal.
AA5086−O	4.12	0.45	0.03	0.10	0.24	0.34	Bal.

Table 2 Mechanical properties of parent materials

Alloy	Yield strength/MPa	Ultimate tensile strength/MPa	Average hardness (HV)
AA6061−T6	260	300	105
AA5086−O	112	250	65

Table 3 Welding condition and process parameters

Parameter	AA6061 with AA6061	AA5086 with AA5086	AA6061 with AA5086
Tool rotational speed/(r·min^{-1})	1300	500	500
Tool traverse speed/(mm·min^{-1})	35	5	10
Axial force/kN	6.0	4.3	4.9
Tool pin profile	Cylindrical taper threaded	Cylindrical plain taper	Cylindrical plain taper
Tool shoulder diameter/mm	18	18	18
Tool pin diameter/mm	5−6	5−6	5−6
Tool pin length/mm	5.7	5.7	5.7
Tool material	High speed steel	High speed steel	High speed steel
Tool inclination/(°)	0	0	0

3 Results

3.1 Macrostructure

Figure 2 shows the cross sectional macrographs of the S66, S55 and D65 joints. The onion ring formation is observed in the weld nugget region of S66 joints (Fig. 2(a)). Figure 2(b) shows the inverted trapezoid shaped stir zone in S55 joint. The annular volume of stir zone is higher than the other macrographs because of relatively high yielding of the material. D65 joint shows a complex meshing of materials (Fig. 2(c)). The material mixing and mechanical interlocking of the material AA6061 (advancing side) with AA5086 (retreating side) is clearly observed.

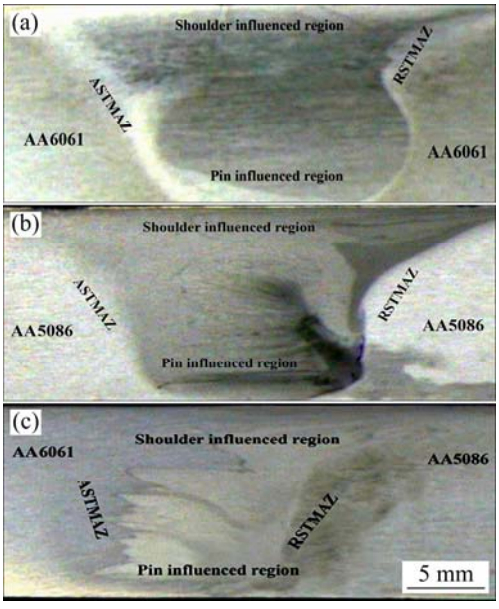

Fig. 2 Macrographs of joint cross section: (a) S66; (b) S55; (c) D65

3.2 Microstructure

The parent metal (AA6061) shows coarser elongated microstructure in which the grains are oriented along the rolling direction (Fig. 1(a)). The dark spots reveal etch pits in the microscope due to over etching. The grains are slightly oriented in the rolling direction. Figure 1(b) shows the base material microstructure of AA5086 aluminium alloy. The grains are marginally smaller than that of AA6061 aluminium alloy and etch pits are found in the microstructure. Figure 3 shows the microstructures of shoulder influenced and pin influenced regions of FSW joints. In S66 and S55 joints, the shoulder influenced region shows larger grain size than the pin influenced region. The downward flow of material is observed in the shoulder influenced region and lamellar flow of materials were observed in the D65 joint (Figs. 3(e) and 3(f)). A clear interface was observed

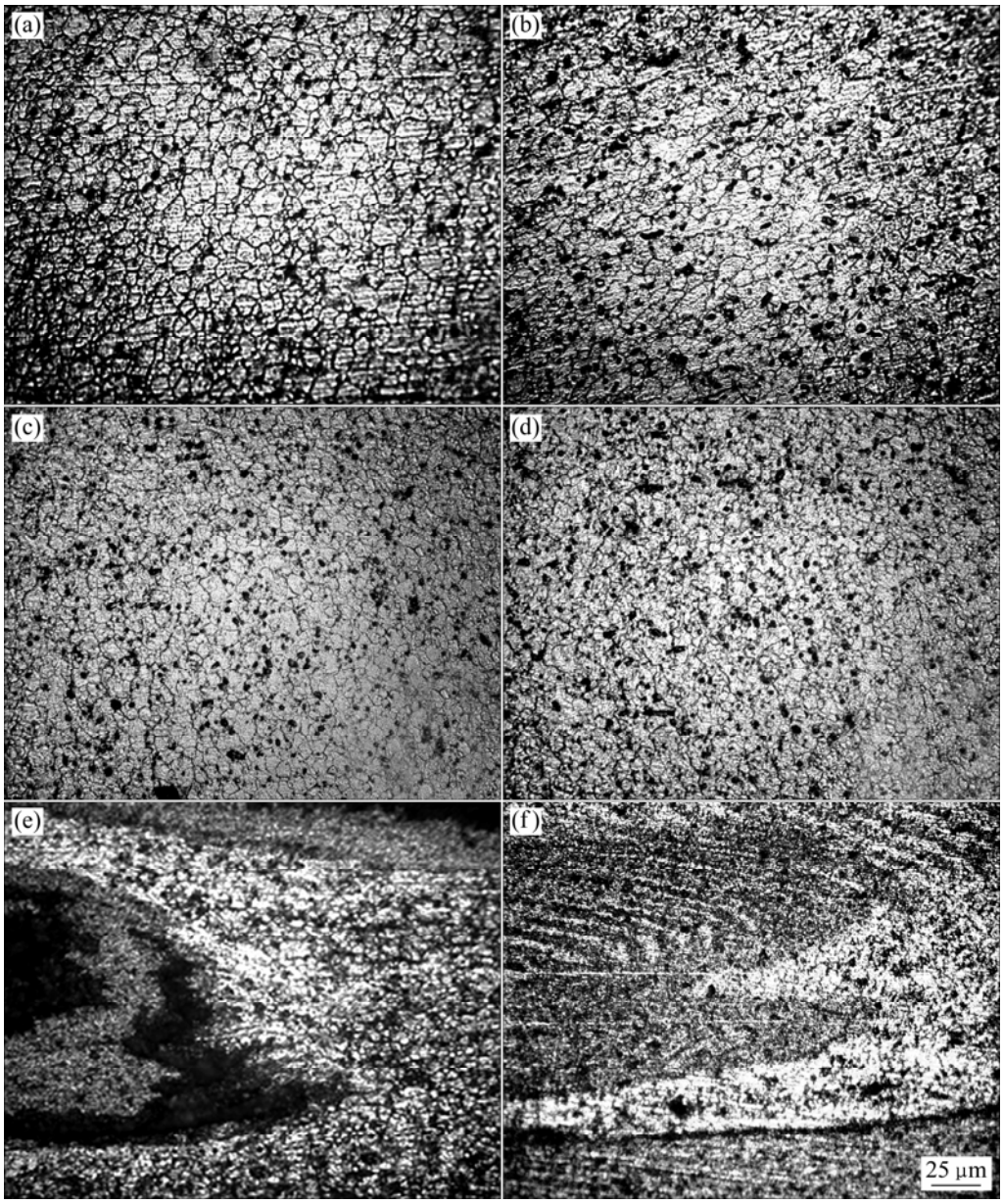

Fig. 3 Optical microstructures of stir zone region FSW joints: (a) S66, shoulder influenced region; (b) S66, pin influenced region; (c) S55, shoulder influenced region; (d) S55, pin influenced region; (e) D65, shoulder influenced region; (f) D65, zone region pin influenced region

Table 4 Tensile properties of FSW joints

Joint type	Yield strength/ MPa	Tensile strength/ MPa	Elongation in 50 mm gauge length/%	Notch tensile strength/MPa	Notch strength ratio	Joint efficiency/ %
S66	180	222	9.0	240	1.08	74
S55	150	180	7.0	203	1.12	72
D65	120	140	5.5	136	0.97	56

between the stir zone and thermo-mechanical affected zone (TMAZ) region of S66, S55 and D65 joints (Fig. 4). The size of TMAZ region is wider and the grains are greatly deformed downwards in the S55 and D65 joints than S66 joint. The grain size is decreased gradiently towards the stir zone.

3.3 Tensile properties

Figure 5 shows the photographs of specimen before and after the tensile test. In each condition, three

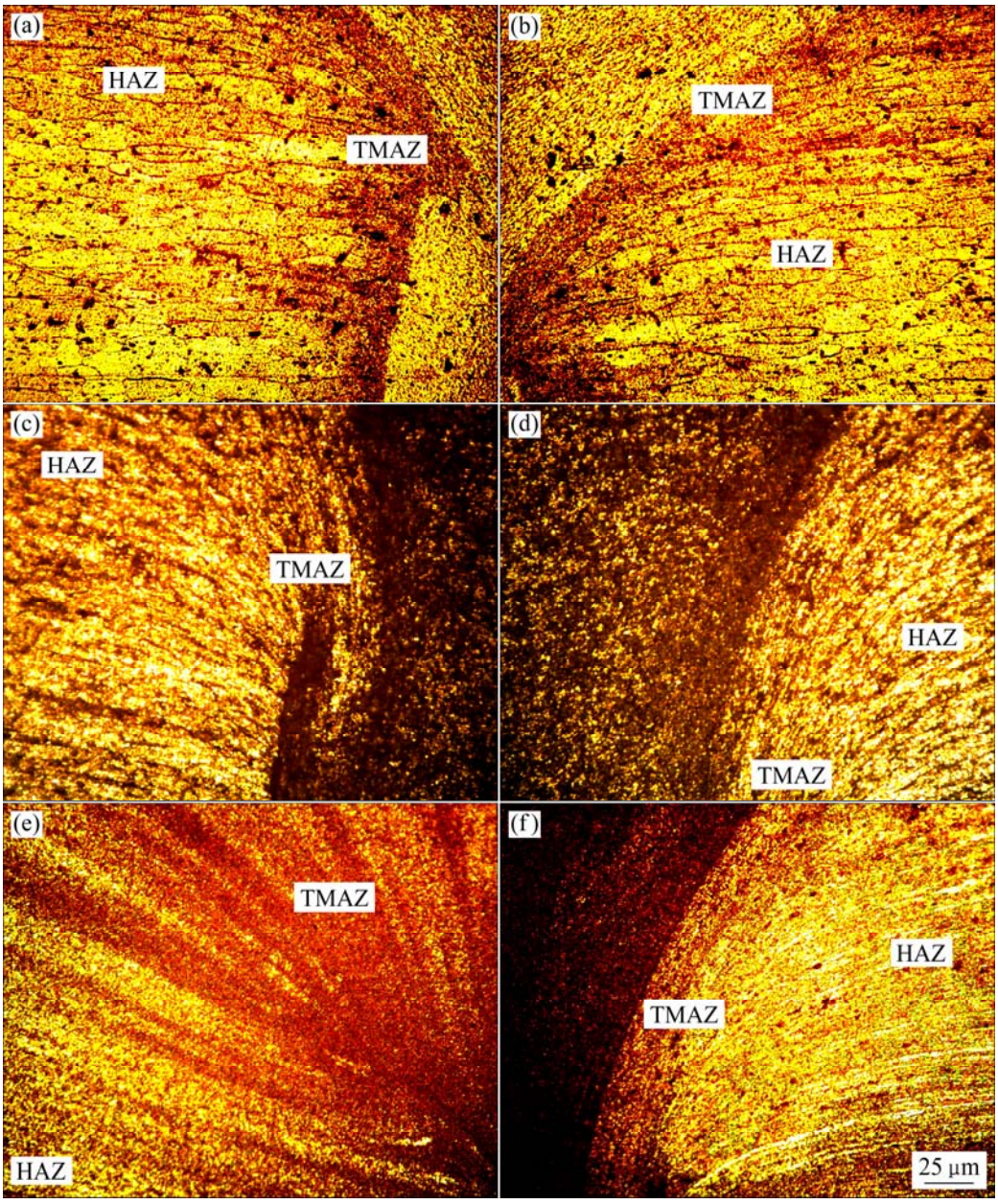

Fig. 4 Optical micrographs of interface region of FSW joints: (a) S66, advancing side; (b) S66, retreating side; (c) S55, advancing side; (d) S55, retreating side; (e) D65, advancing side; (f) D65, retreating side

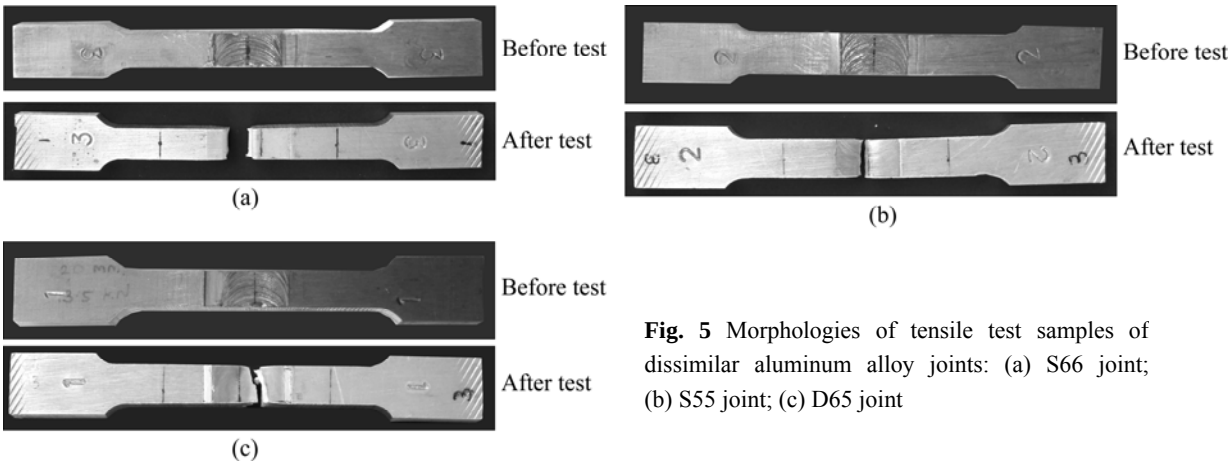

Fig. 5 Morphologies of tensile test samples of dissimilar aluminum alloy joints: (a) S66 joint; (b) S55 joint; (c) D65 joint

specimens were tested and the average values are accounted for the analysis (Table 4). The tensile strength of friction stir welded similar AA6061 Al joint (S66) is 222 MPa which is 74% of base metal Al alloy. The tensile strength of S55 joint is 180 MPa, which is 28% lower than the parent metal AA5086. The tensile strength of D65 joint is 140 MPa, which is 36% lower than that of the AA5086 alloy joint and 30% lower than that of AA6061 alloy joint. The tensile strength of the dissimilar joint was lower than that of the similar joint and lower than that of both the parent materials. The elongations (ductility) of the friction stir welded S66 and S55 alloy joints are 9% and 7% respectively. The D65 joint shows relatively low ductility of 5.5%. The notch strength ratio (NSR, ratio between notch tensile strength and tensile strength) is calculated for S66 and S55 as 1.01 and 1.19, respectively. Since NSR is greater than 1.0, these two joints fall under notch ductile material category, i.e., the joint strength is higher in notched condition than in unnotched condition. However, the NSR of friction stir welded D65 joint is 0.97 which is lower than 1.0 and hence dissimilar joint falls under "notch brittle material" category, i.e, the joint strength is lower in notched condition than in unnotched condition. This parameter is also one of the useful measurements to evaluate ductility of the materials. The joint efficiency is calculated and shown in Table 4. The joint efficiency of S66 joints is 74% which is relatively higher than the counterparts. Minimum joint efficiency of 56% is observed for the dissimilar joints. The joint efficiency of S55 is 72%, almost equal to S66 joints. Figure 6 shows the stress−strain curve for smooth tensile specimen. S66 joint exhibits relatively higher tensile strength with maximum strain than other joints. D65 joint exhibits poor tensile strength and strain compared to similar joints. The heterogeneous microstructure in the stir zone creates a heterogeneous stress distribution which results in the lower stress−strain characteristics.

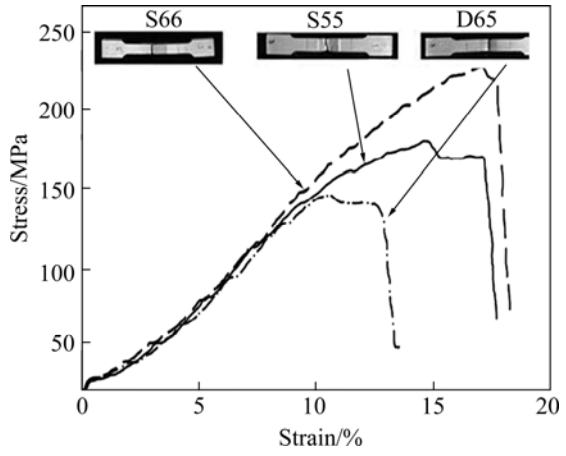

Fig. 6 Stress−strain curves of dissimilar aluminum alloy joints

3.4 Fractograph

Figures 7 and 8 show the fracture surface of tensile test specimens at lower and higher magnifications. Fine populated dimples were observed in S66 joint (Fig. 7(a)) at the higher magnification which resembles ductile mode of the failure. A quasi state cleavage and few dimples were observed in the S55 joint (Fig. 7(b)). D65 joint shows the fine dimples at the shoulder influenced region and cleavage like fracture in the pin influenced region (Fig. 7(c)). The fracture surface of notched sample specimens shows larger dimples than the smooth specimen. In D65 joint, cleavage facet was observed along with the tear ridges (Fig. 8(c)).

3.5 Microhardness

Figure 9 shows the hardness profile measured across the weld at the mid-thickness region of S66, S55 and D65 joints. It is clearly evident that there is a larger variance in the hardness values in the stir zone of the D65 joint. The microhardness curve shows a W-shape profile for S66 joint with the maximum hardness value of HV 115. S55 joint shows the lower hardness values than the S66 joint (HV 74 at the stir zone). A hardness loss is observed on the advancing side and retreating side TMAZ region of both S66 and S55 joints. D65 joint shows the decreasing trend from the advancing side to the retreating side. AA6061 alloy is placed on the advancing side and AA5086 alloy is placed in the retreating side. The base material hardness of AA6061 alloy is reduced towards the stir zone to HV 68 in D65 joints and further decreased to HV 65 towards AA5086 alloy side.

4 Discussion

The results of this work show that FSW can produce defect-free butt welds between AA6061 and AA5086 plate material, demonstrating the unique capabilities of the process in dealing with joining of dissimilar aluminium alloys. In friction stir welding, the joining of materials is achieved by the heat generation due to the rubbing of the tool with the work piece and plastic deformation, i.e., material flow. The generated heat is utilized to soften the column of materials which favours the material flow. During welding, the material is excavated from advancing side to the retreating side at the front end of the tool and the materials are transported from retreating side to advancing side at the tool rear end. When the material is excavated from advances side, it creates a vacancy. During the rotation of the tool, the material from retreating side should fill the vacancy created in the advancing side, if the amount of material transported to advancing from retreating side is less than

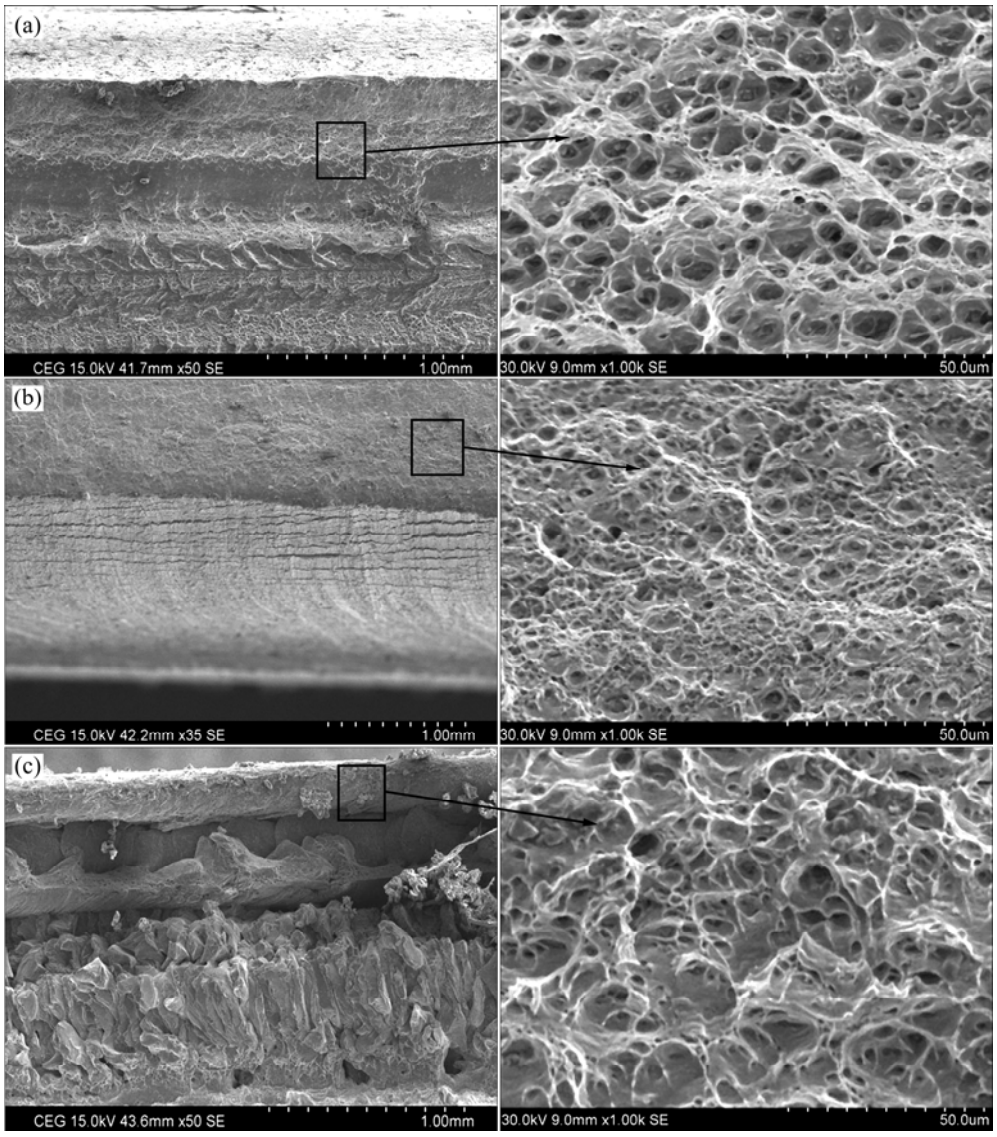

Fig. 7 Fractrographs of smooth tensile specimens: (a) S66; (b) S55; (c) D65

the amount of material excavate from the advancing. If the heat generation is low, the material plasticization is low which in turn results in poor material flow. This results in defect in the stir zone. On the other hand, if the heat generation is excess, turbulent flow of materials occurs which in turn also results in a defect. Thus the optimum heat generation is needed to achieve the defect free joint. Despite of the optimum heat generation, the material should be directed by the pin profile to results defect free joint. The shoulder influenced region is defined as the top portion of stir region which experienced the effects like heat generation and material flow which are solely created by the rotation and rubbing of tool shoulder during FSW. The pin influenced region is defined as the bottom portion of stir region, which experiences the effects like heat generation and material flow, which are solely created by the rotation and rubbing of the tool pin during FSW. In special, the strengths of these dissimilar materials mainly concern on the mechanical interlocking of materials, thus the materials should be flowed and mixed properly. Thus materials flow decides the formation of defect free stir zone and strength of the dissimilar joint.

S66 joint exhibited relatively higher tensile strength than S55 and D65 joints. The fracture was observed in the TMAZ region. The thermal cycle prevailed in the TMAZ region leads to the dissolution of precipitates, which make the region softer. The loss in strength is also attributed to the lower hardness. During tensile loading, the fracture in the tensile tests occurred in the soft region, which happened to be the weakest point of the specimen [22,23]. However, in dissimilar joints, the strength of the joint is mainly attributed to the mechanical interlocking of the materials rather than metallurgical bonding. Thus,

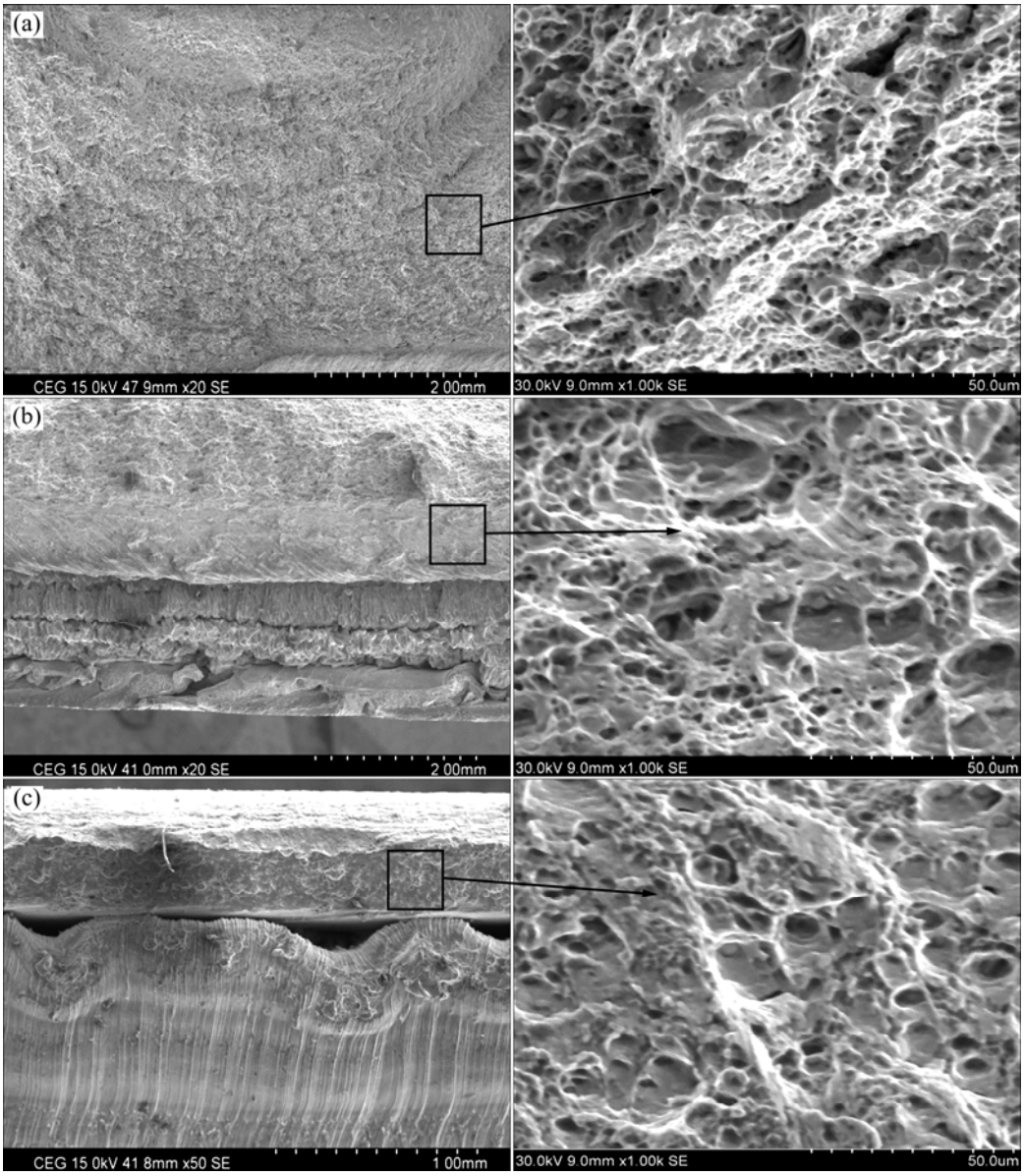

Fig. 8 Fractrographs of notched tensile specimens: (a) S66; (b) S55; (c) D65

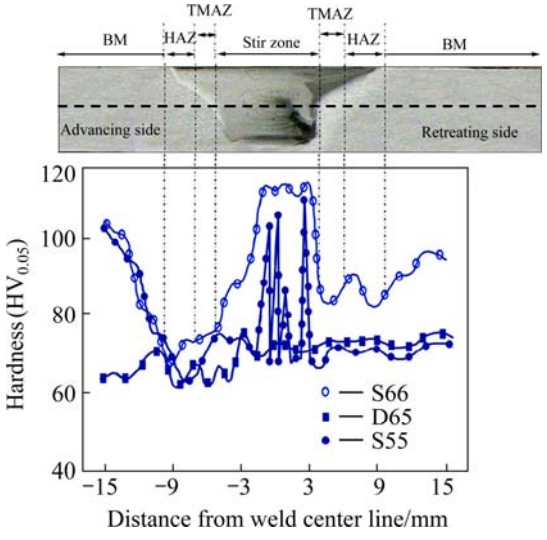

Fig. 9 Hardness profile across weld

the dissimilar joints show relatively lower tensile properties than the other two similar joints. The macrostructure of dissimilar joint is characterized by the complex solid-state flow and mixing of the materials. The features like chaotic flow, interpenetrating features and the longer interface layer increase the mechanical interlocking which results in improved tensile properties [24]. These features were not observed in the D65 joint (Fig. 4(c)). This may be one of the reasons for the lower strength of D65 joint than the S66 and S55 joints.

The tensile fracture surfaces at low and high magnifications were investigated. The lower and higher magnifications of S66 and S55 joints (Figs. 7(a), 7(b), 8(a) and 8(b)) show fine populated dimples which are the characteristic features of ductile mode of failure. The center of the dimples shows a hole like appearance which

acts as the fracture initiation sites. For the dissimilar joint D65, the fracture area close to the crown shows fine dimples and the fracture area close to pin influenced region shows the transgranular cracking of the brittle intermetallic phases (Fig. 7(c)) and the step like fracture surface similar in appearance to cleavage facets (Fig. 8(c)).

Figures 3 and 4 show the grain size variation in different regions of FSW joints. The heat generation due to friction between the tool and workpiece interface and due to plastic deformation of the fine equi-axed grains is formed in the stir zone of all the joints. The shoulder influenced region exhibits higher heat generation which allows the grains to grow. This results in larger grain size than pin influenced region. The material flow downwards by the aid of axial force at the shoulder influenced region and lamellar structure of AA6061 and AA5086 is formed due to the stirring of both materials in the pin influenced region (Fig. 3(d)). This is evident that the proper stirring of material was done to make the defect free joint. The heterogeneous microstructure in the dissimilar joint exhibits non-homogeneous plastic deformation across the joint during tensile loading. This difference induced variation in the stress patterns, which leads D65 joint to fail earlier. STEUWER et al [25] reported that the uneven distribution of heat during welding induced stress gradients along the joint which affect the tensile properties of FSW joints.

The hardness of the FSW joint is based upon the hard, brittle intermetallic formation, boundary energy, precipitate formation and strain hardening in the joint. The increase of grain boundaries and fine grains in the stir zone of S66 joints shows higher hardness. From the Hall-Petch relationship, it was understood that the grain size is inversely proportional to the hardness and strength. Hence, the formation of fine recrystallized grains results in higher hardness in the stir zone. Due to high tool rotation speed, the high heat is generated in the S66 joints. This shows relatively large grain size than the counterparts. This will result in lower hardness. Despite the fact, for the age hardenable alloys, rather than grain size, the precipitates formation shows significant effect on the mechanical properties. During welding, the heat generated in the stir zone is conducted to the neighbouring regions (TMAZ and HAZ). For the heat treatable aluminium alloy, the strength and hardness mainly depends on the availability and distribution of the precipitates. The availability and distribution of precipitates in the matrix are controlled by the prevailing thermal conditions. The precipitation sequence of Al−Mg−Si 6xxx alloys is generally described to be: solid solution→ GP → β'' → β'→ β (Mg_2Si). During solutionization, the precipitates are dissolved in the matrix and form super saturated solid solution upon cooling. Further aging leads to the precipitation of a secondary phase which reinforces the strength of aluminum alloy [26]. Since AA6061 is a heat treatable aluminium alloy, the hardness is mainly attributed to the presence of precipitates. The thermal cycle prevailed in the ASTMAZ region creates the dissolution of strengthening precipitates which shows reduced hardness values in the Fig. 9. This region is softer because the solute additions trapped in second phases dissolve back into solid solution. In other word, the heating and cooling thermal condition prevails in the TMAZ, making the precipitates dissolve in the matrix. The non-heat treatable alloy joint S55 shows improved hardness in the stir zone due to the work hardening effect. The strain hardened stir zone resists further deformation (indentation) and improves the hardness values. The erratic hardness spikes are observed in the stir zone of D65 joint. This is an indication that the intercalated DRX bands or shear bands contain heavily deformed DRX regimes intermixed with the softer and relative dislocation free DRX zones [27]. The microhardness distribution in the weld was uneven and erratic hardness spikes exhibiting hardness values as much as three times that of the base material was already reported in literature [28,29]. At the interface of the dissimilar materials, due to the diffusion of chemically incompatible dissimilar materials, the intermetallic compounds formed. The intermetallics are hard and brittle in nature. Thus, at the interface of dissimilar materials in the stir zone, the D65 joint shows higher hardness. The stir zone is a heterogeneous system composed of mixing of materials and staking of materials into lamella layers. Thus, this results in uneven hardness distribution in the stir region. The results are confirmed from the previous literatures [30−32].

5 Conclusions

1) The tensile strength of D65 joints is 140 MPa, which is 30% lower than that of S66 joint and 34% lower than that of S55 joint.

2) An improved hardness of HV 115 is obtained in the stir zone, which is higher than the parent metals hardness. Higher grain boundary fraction and formation of brittle intermetallic phases at the weld improve the hardness.

Acknowledgement

The authors gratefully acknowledge the support extended by the Centre for Materials Joining & Research (CEMJOR), Department of Manufacturing Engineering,

Annamalai University, Annamalai Nagar, India to carry out this research.

References

[1] JAMSHIDI AVAL H, SERAJZADEH S, KOKABI A H. Evolution of microstructures and mechanical properties in similar and dissimilar friction stir welding of AA5086 and AA6061 [J]. Materials Science and Engineering A, 2011, 528: 8071−8083.

[2] SAKANO R, MURAKAMI K, YAMASHITA K, HYOE T, FUJIMOTO M, INUZUKA M. Development of spot FSW robot system for automobile body members [C]// Proceedings of the 3rd International Symposium of Friction Stir Welding. Kobe, Japan, 2001: 27−28.

[3] LUIJENDIJK T. Welding of dissimilar aluminium alloys [J]. Journal of Materials Processing Technology, 2000, 103: 29−35.

[4] YAN Yong, ZHANG Da-tong, QIU Cheng, ZHANG Wen. Dissimilar friction stir welding between 5052 aluminum alloy andAZ31 magnesium alloy [J]. Transactions of Nonferrous Metals Society of China, 2010, 20(4): 619−623.

[5] KOILRAJ M, SUNDARESWARAN V, VIJAYAN S, KOTESWARA RAO S R. Friction stir welding of dissimilar aluminum alloys AA2219 to AA5083–Optimization of process parameters using Taguchi technique [J]. Journal of Materials Science, 2012, 42: 1−7.

[6] XUE P, NI D R, WANG D, XIAO B L, MA Z Y. Effect of friction stir welding parameters on the microstructure and mechanical properties of the dissimilar Al−Cu joints [J]. Materials Science and Engineering A, 2011, 528: 4683−4689.

[7] MISHRA R S, MA Z Y, Friction stir welding and processing [J]. Materials Science and Engineering R, 2005, 50: 1−78.

[8] KWON Y J, SHIGEMATSU I, SAITO N. Dissimilar friction stir welding between magnesium and aluminum alloys [J]. Materials Letters, 2008, 62:3827–3829.

[9] CHEN Yu-hua, NI Quan, KE Li-ming. Interface characteristic of friction stir welding lap joints of Ti/Al dissimilar alloys [J]. Transactions of Nonferrous Metals Society of China, 2012, 22(2): 299−304.

[10] KWON Y J, SHIM S B, PARK D H. Friction stir welding of 5052 aluminum alloy plates [J]. Transactions of Nonferrous Metals Society of China, 2009, 19(s1): s23−s27.

[11] MOFID M A, ABDOLLAH-ZADEH A, MALEK GHAINI F. The effect of water cooling during dissimilar friction stir welding of Al alloy to Mg alloy [J]. Materials and Design, 2012, 36: 161−167.

[12] XUE P, XIE G M, XIAO B L, MA Z Y, GENG L. Effect of heat input conditions on microstructure and mechanical properties of friction-stir-welded pure copper [J]. Metallurgical and Materials Transactions A, 2010, 41(8): 2010−2021.

[13] SPRINGER H, KOSTKA A, DOS SANTOS J F, RAABE D. Influence of intermetallic phases and Kirkendall-porosity on the mechanical properties of joints between steel and aluminium alloys [J]. Materials Science and Engineering A, 2011, 528: 4630−4642.

[14] CAVALIERE P, PANELLA F, Effect of tool position on the fatigue properties of dissimilar 2024−7075 sheets joined by friction stir welding [J]. Journal of Material Processing Technology, 2008, 206: 249−255.

[15] BAHEMMAT P, HAGHPANAHI M, BESHARATI M K, AHSANIZADEH S, REZAEI H. Study on mechanical, micro and macrostructural characteristics of dissimilar friction stir welding of AA6061−T6 and AA7075−T6 [J]. Journal of Engineering Manufacture, 2010, 224: 1854−1864.

[16] HECTOR L G Jr, CHEN Y L, AGARWAL S, BRIANT C L. Friction stir processed AA5182−O and AA6111−T4 aluminum alloys. Part 2: Tensile properties and strain field evolution [J]. Transactions of Nonferrous Metals Society of China, 2007, 16(4): 404−417.

[17] KHODIR S A, SHIBAYANAGI T. Friction stir welding of dissimilar AA2024 and AA7075 aluminum alloys [J]. Materials Science and Engineering B, 2008, 148: 82−87.

[18] CAM G, GUCLUER S, CAKAN A, SERINDAG H T. Mechanical properties of friction stir. butt-welded Al−5086 H32 plate [J]. Materialwissenschaft und Werkstofftechnik, 2009, 40(8): 638−642.

[19] HEIDARZADEH A, KHODAVERDIZADEH H, MAHMOUDI A, NAZARI E. Tensile behavior of friction stir welded AA6061−T4 aluminum alloy joints [J]. Materials and Design, 2012, 37: 166−173.

[20] LIU H J, HOU J C, GUO H. Effect of welding speed on microstructure and mechanical properties of self-reacting friction stir welded 6061−T6 aluminum alloy [J]. Materials and Design, 2013, 50: 872−878.

[21] ÇAM G, GÜÇLÜER S, ÇAKAN A, SERINDAĞ H T. Mechanical properties of friction stir butt-welded Al−5086 H32 plate [J]. Journal of Achievements in Materials and Manufacturing Engineering, 2008, 30(2), 151−154.

[22] SCIALPI A, de GIORGI M, de FILIPPIS L A C, NOBILE R, PANELLA F W. Mechanical analysis of ultra-thin FSW joined sheets with dissimilar and similar materials [J]. Materials and Design, 2008, 29: 928−36.

[23] MOREIRA P M G P, SANTOS T, TAVARES S M O, RICHTER-TRUMMER V, VILAÇA P, DE CASTRO P M S T. Mechanical and metallurgical characterization of friction stir welding joints of AA6061−T6 with AA6082−T6 [J]. Materials and Design, 2009, 30: 180−187.

[24] VENKATESWARAN P, REYNOLDS A P. Factors affecting the properties of friction stir welds between aluminum and magnesium alloys [J]. Journal of Materials Engineering and Performance, 2012, 545: 26−37.

[25] STEUWER A, PEEL M J, WITHERS P J. Dissimilar friction stir welds in AA5083−AA6082: The effect of process parameters on residual stress [J]. Materials Science and Engineering A, 2006, 441: 187−196.

[26] GALLAIS C, DENQUIN A, BRÉCHET Y, LAPASSET G. Precipitation microstructures in an AA6056 aluminium alloy after friction stir welding: Characterisation and modeling [J]. Materials Science and Engineering A, 2008, 496: 77−89.

[27] SOMASEKHARAN A C, MURR L E. Microstructures in friction-stir welded dissimilar magnesium alloys and magnesium alloys to 6061−T6 aluminum alloy [J]. Materials Characterization, 2004, 52: 49−64.

[28] ZETTLER R. Dissimilar Al to Mg alloy friction stir welds [J]. Advanced Engineering Materials 2006, 8(5): 415−421.

[29] MURR L E, YING L I, FLORES R D, ELIZABETH TRILLO A, MCCLURE J C. Intercalation vortices and related microstructural features in the friction-stir welding of dissimilar metals [J]. Materials Research Innovations, 1998, 2(3): 150−163.

[30] SHIGEMATSU I, KWON Y J, SUZUKI K, IMAI T, SAITO N. Joining of 5083 and 6061 aluminum alloys by friction stir welding [J]. Journal of Materials Science Letters, 2003, 22: 353−356.

[31] POUYA B, MOHAMMAD H, MOHAMMAD K B G, KAMBIZ R S. Study on dissimilar friction stir butt welding of AA7075−O and AA2024−T4 considering the manufacturing limitation [J]. International Journal of Advanced Manufacturing Technology, 2012, 59: 939–953.

[32] MURR L E. A review of FSW research on dissimilar metal and alloy systems [J]. Journal of Materials Engineering and Performance, 2010, 19(8): 1071−1089.

搅拌摩擦焊异种 AA6061-AA5086 铝合金接头的显微组织与力学性能

M. ILANGOVAN[1], S. RAJENDRA BOOPATHY[1], V. BALASUBRAMANIAN[2]

1. Department of Mechanical Engineering, College of Engineering Guindy, Anna University, Chennai, India;
2. Center for Materials Joining & Research, Department of Manufacturing Engineering, Annamalai University, Annamalai Nagar Chidambaram 608002, Tamilnadu, India

摘　要：在熔焊异种可热处理强化和不可热处理强化铝合金过程中，面临许多与凝固相关的问题。采用搅拌摩擦焊接可以解决这些问题，从而可以综合利用两种铝合金的优异性能。研究搅拌摩擦焊同种和异种 AA6061 和 AA5086 焊接接头的显微组织和拉伸性能。采用光学显微镜和扫描电子显微镜观察分析不同区域的显微组织，测量焊接接头不同部位的显微硬度，评价焊接接头的拉伸性能，并研究其与显微组织和显微硬度之间的关联。研究发现，异种焊接接头的最大维氏硬度为 HV 115，焊接效率为 56%。这主要是由于获得无缺陷的搅拌区和晶粒增强作用。

关键词：搅拌摩擦焊；异种接头；铝合金；显微组织；拉伸强度

(Edited by Yun-bin HE)